Journal of Materials Chemistry A

Accepted Manuscript

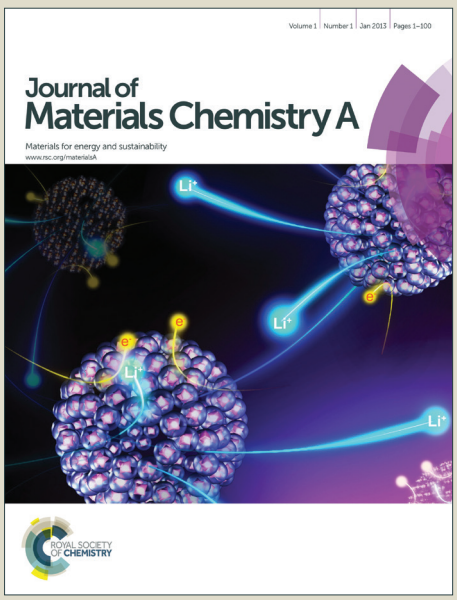

ROYAL SOCIETY OF CHEMISTRY

www.rsc.org/materialsA

Journal of Materials Chemistry A RSCPublishing

COMMUNICATION

Efficient Planar-Heterojunction Perovskite Solar Cells Achieved via Interfacial Modification of Sol-gel ZnO Electron Collection Layer

Cite this: DOI: 10.1039/xoxxoooooox

Received ooth January 2014,
Accepted ooth January 2014

DOI: 10.1039/xoxxoooooox

www.rsc.org/

Junghwan Kim,[a] Geunjin Kim,[b] Tae Kyun Kim,[c] Sooncheol Kwon,[a] Hyungcheol Back,[b] Jinho Lee,[a] Seoung Ho Lee,[c] Hongkyu Kang[b] and Kwanghee Lee[*a,b,c]

The importance of interfacial engineering as a new strategy for improving the power conversion efficiencies (PCEs) of planar-heterojunction (PHJ) perovskite solar cells is highlighted in this study. With our optimized interfacial modification, we demonstrated efficient PHJ perovskite solar cells with a high PCE of 12.2% using a sol-gel-processed ZnO ECL modified by [6,6]-phenyl C_{61} butyric acid methyl ester (PCBM).

The recent tremendous progress in thin-film solar cell technology using solution-processable organic-inorganic hybrid perovskites-such as $CH_3NH_3PbX_3$ (X = Cl, Br, I)-is an important milestone in the field of renewable solar devices.[1-6] Because hybrid organic-inorganic methylammonium lead halide perovskites exhibit excellent semiconducting properties, such as high charge-carrier mobility (~10 cm^2 $V^{-1}s^{-1}$), a direct band gap (~ 1.5 eV), a broad absorption range, a small exciton binding energy (~ 20 meV), and a long-range exciton diffusion length (100 ~ 1000 nm), the new family of solar cells incorporating hybrid light-harvesting materials is expected to achieve power conversion efficiencies (PCEs) of up to 20% in the near future.[4, 6]Motivated by the great potential of organometal halide perovskites, intensive studies have been conducted on the charge dynamics of perovskites,[5, 6] synthesis of new materials,[7] optimization of perovskite absorber layers by increasing crystallinity[4, 8] and surface coverage,[9] and realization of low-temperature processed devices [10-12]over the past several years.

Recently, studies on planar-heterojunction (PHJ) perovskite solar cells, sandwiched between the hole transport layer (HTL) and the electron collection layer (ECL) without mesoporous scaffolds, have attracted much attention due to their simplified fabrication process and compatibility with roll-to-roll processing on flexible substrates.[1, 8] To realize the PHJ perovskite solar cells, several nano-sized TiO_2 or ZnO nanoparticles (NPs) have been used as compact ECLs in the devices.[3] However, the NPs are usually synthesized by relatively complex procedures including long reaction time, precipitation, washing, and dilution processes.[13] In addition, ligand-linked NPs need a high temperature annealing process, which is incompatible with flexible substrates, and ligand-free NPs usually suffer from poor dispersion stability.[14, 15] In contrast, sol-gel processed metal oxides have many advantages of simple synthesis, long-term stability, solution, and low temperature processability and are more suitable for printable photovoltaics.[16]

Nevertheless, there are few reports to successfully demonstrate efficient PHJ perovskite solar cells by incorporating the sol-gel metal oxides. In addition, although the interfacial engineering of the interface between electrodes and the light absorber films has been one of the most important strategies for improving the PCEs of thin-film solar cells, only few reports on this method in the field of PHJ perovskite solar cells have been published. Therefore, the aim of this work was to replace the complicated NPs with simple sol-gel compact ECLs and to study the effect of the interfacial modification of

the sol-gel processed ECLs on device performance by analyzing the electronic structures of the interfacial layers and perovskite absorber for optimizing the device performance of PHJ perovskite solar cells.

In this communication, we successfully demonstrate efficient PHJ perovskite solar cells with a sol-gel processed ZnO ECL modified by a thin organic surface modifier, [6,6]-phenyl C_{61} butyric acid methyl ester (PCBM). By depositing PCBM onto the sol-gel ZnO, the electronic structure of the ZnO could be modulated, and the V_{oc} values of the devices containing the ZnO/PCBM were enhanced compared to those of the devices containing only ZnO. In addition, the interfacial modification of ZnO was observed to significantly reduce trap-assisted charge recombination at the interface of ZnO as well as in the bulk of the perovskite absorber, thereby improving the device performance. With our optimized interfacial modification, we demonstrated efficient PHJ perovskite solar cells with a PCE of 12.2% using a sol-gel-processed ZnO/PCBM ECL.

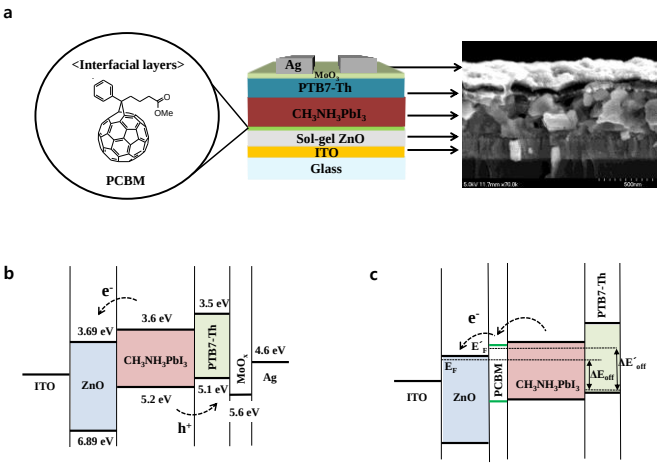

Figure 1. (a) The device structure of the planar-heterojunction perovskite solar cells and the molecular structures of the interfacial layers PCBM. A cross-sectional SEM image of the device is also shown. Energy-level diagram of the components of the perovskite solar cells (b) without and (c) with the PCBM. The energy-level offset (ΔE_{off}) is the energy-level difference between the quasi Fermi levels of the electron collection layer and the hole transport layer.

Figure 1a illustrates the device architecture of the PHJ perovskite solar cells and the chemical structures of the organic interfacial modifier PCBM used in this work. The device structure is ITO/ZnO/$CH_3NH_3PbI_3$/PTB7-Th/MoO_3/Ag, where the perovskite film ($CH_3NH_3PbI_3$) was grown using a sequential deposition method to achieve a good film coverage and crystallization (see supporting information S1).[2] The results of a structural investigation of PbI_2 and $CH_3NH_3PbI_3$ using a selected area electron diffraction (SAED) clearly show that the phase of PbI_2 (hexagonally closed-packed layer) was successfully transformed into the perovskite structure of $CH_3NH_3PbI_3$ (see supporting information S2).

To selectively extract electrons from the $CH_3NH_3PbI_3$ absorber, a 30-nm-thick sol-gel-processed ZnO layer was deposited onto the ITO electrode as the ECL. The sol-gel ZnO film offers several advantages including easy solution processability, air stability, excellent optical transparency, good film formation, and relatively low-temperature processability. Furthermore, because the sol-gel ZnO has much higher electron mobility than that of titanium oxide, it is an ideal material as an ECL for the PHJ perovskite solar cells. [16] For the interfacial modification of the top surface of the ZnO layer, PCBM were spin-coated onto the ZnO film and then annealed at 80 °C for 5 min. Because the fullerene derivative of the PCBM is an excellent electron acceptor having favorable electronic structure with respect to the perovskite absorber, it is expected that the modifiers can effectively modulate the interfacial properties of ZnO.[17] Scanning electron microscopy (SEM) and atomic force microscopy (AFM) measurement show that the ZnO and the ZnO/PCBM films have a very smooth and compact morphology (Figure S3 and S4).

In our perovskite solar cells, we utilized a new class of PBDTTT-type low-band-gap conjugated polymer composed of benzodithiophene (BDT) and thieno[3,4-b]thiophene (TT) units, PTB7-Th, as a HTL.[18] Because the PTB7-Th layer has an excellent hole mobility of 1.5 x 10^{-2} $cm^2V^{-1}s^{-1}$ as well as an appropriate oxidation potential of 5.2 eV, it is expected to function efficiently as a HTL in perovskite solar cells (see supporting information S5). More detailed information regarding the preparation of the perovskite absorber, sol-gel ZnO, and PTB7-Th and the device fabrication is described in the experimental section.

The energy-level diagrams of the component materials and the effect of ZnO interfacial modification are illustrated in Figure 1b and c, respectively. The valence band maximum (VBM) values of the ZnO and the perovskite films were determined by ultraviolet photoelectron spectroscopy (UPS), and the conduction band minimum (CBM) values were calculated by adding the optical band gap (E_g) derived from the UV-visible absorption onset (Figure S6). The spectroscopic measurements show that the ZnO film has a VBM of 6.89 eV and a CBM of 3.69 eV, respectively. The electronic structure of PTB7-Th was obtained from the literature.[18] Because the CBM (3.60 eV) and VBM (5.20 eV) of the perovskite film are close to those of the ZnO and PTB7-Th layers, respectively, the efficient charge extraction (or dissociation) of free charge carriers (or excitons) generated in the perovskite film is expected, as shown in Figure 1b. It is noteworthy that a stable molybdenium oxide (MoO_x) thin film was deposited on top of the PTB7-Th HTL in our perovskite solar cells. Because the TMO interlayer helps to extract holes more efficiently, we obtained dramatically enhanced device performance by introducing the MoO_x interlayer (see supporting information Figure S7). The role of MoO_x layer is to reduce contact resistance at the interface of HTL and Ag electrode by hole-doping of the organic HTL with the MoO_x.[19, 20] Therefore, we

expect that various new types of organic materials can be successfully applied to perovskite solar cells as efficient HTLs by combining them with a MoO_x interlayer.

To enhance the efficiency of perovskite solar cells, improving electron transport/extraction is also very important. Therefore, we intended to modify the surface of the ZnO film by incorporating PCBM for better electron transport/extraction between the ZnO and the perovskite absorber. In addition, as shown in Figure 1c, because the V_{oc} of the 'p-i-n' perovskite solar cells is usually determined by the energy-level offset (ΔE_{off}) between the quasi Fermi levels of the ECL and the HTL adjacent to the perovskite absorber,[21, 22] it is expected that an enhancement in the V_{oc} values is possible by changing the electronic structure of the ZnO film using surface modifier, thereby improving device performance.

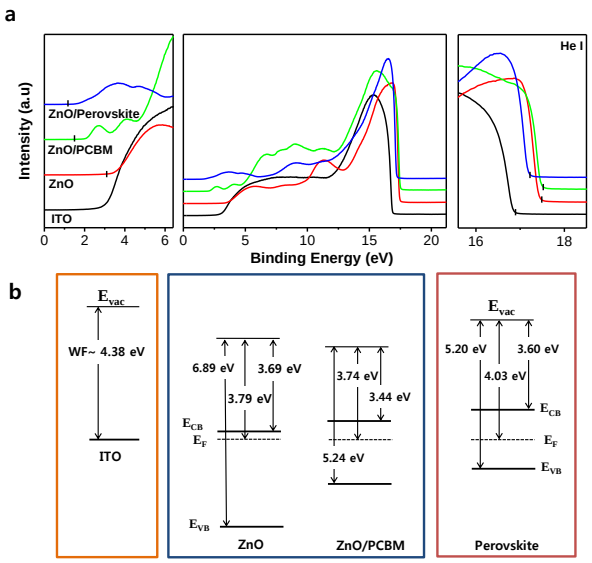

Figure 2. (a) UPS spectra of ITO, ITO/ZnO, ITO/ZnO/PCBM, and ITO/ZnO /perovskite films. (left) the valence band edge, (middle) whole UPS photoemission spectra, and (right) magnified section of the photoemission onset. (b) Energy-level diagrams of the various films resulting from the UPS studies. The Fermi level (E_F) values of each film are aligned due to the thermodynamic equilibrium that arises when they are joined together.

To investigate the electronic structures of the ZnO and ZnO/PCBM, we carried out ultraviolet photoelectron spectroscopy (UPS) measurements. Figure 2a shows the UPS spectra of the ITO, ZnO, ZnO/PCBM, and ZnO/perovskite films. The Photoemission parameters obtained from the UPS measurements are summarized in Table S1. The high binding energy onset of bare ITO is 16.82 eV, yielding a work function (WF) of 4.38 eV. The deposition of a ZnO film on the ITO substrate leads to a shift in the photoemission onset toward higher binding energy (17.41 eV), indicating the formation of an interfacial dipole shifting the vacuum level upward, and the WF decreases to 3.79 eV. The photoemission onset of the ZnO film further shifts toward higher binding energy upon the deposition of the PCBM, decreasing the WF to 3.74 eV. In contrast, the valence band edge ($E_{valence}$) of the ZnO film shifts toward lower binding energy with interfacial modification, shifting the energetic position of the VBM upward with respect to the Fermi level (E_F).

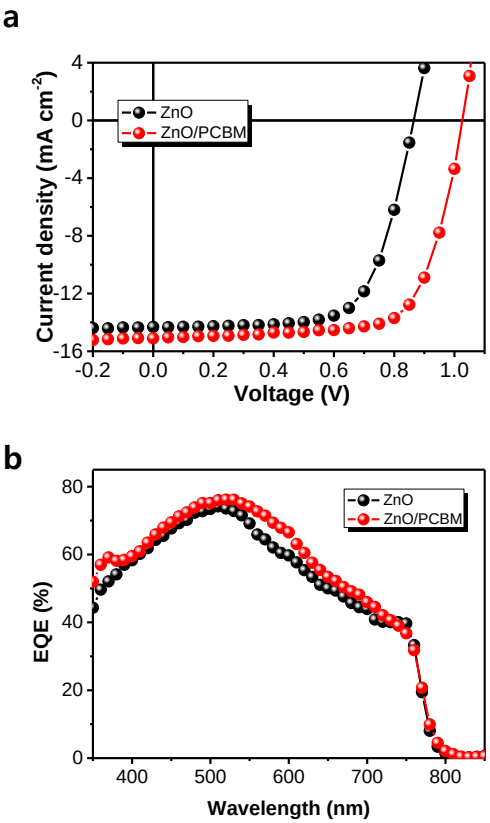

Figure 3. (a) Current density-voltage characteristics of the planar-heterojunction perovskite solar cells incorporating ITO/ZnO and ITO/ZnO/PCBM as cathodes measured under AM 1.5G irradiation at 100 mW cm^{-2}. (b) EQE spectra of the perovskite solar cells.

The electronic structures of the ITO, ZnO, ZnO/PCBM, and ZnO/perovskite films deduced from the UPS measurements are illustrated in Figure 2b. The E_F values of each film are aligned due to thermodynamic equilibrium when they are joined together; band bending is not shown. Because the CBM of the ZnO is lower than that of perovskite, the efficient charge extraction (or dissociation) of free charge carriers (or excitons) generated in the perovskite film is expected. For the ZnO/PCBM ECL, because the CBM of ZnO/PCBM is located between that of ZnO and that of perovskite, much more favorable energy-level alignment occurs at the interfaces, facilitating cascade charge extraction. In addition, the high voltage output of the perovskite solar cell with the ZnO/PCBM layer is expected due to the large energy-level offset between

the quasi Fermi levels of the ECL and the HTL adjacent to the perovskite absorber relative to that afforded by ZnO alone.

To explore the effects of interfacial modification on device performance, we fabricated PHJ perovskite solar cells with a structure of ITO/sol-gel ZnO/$CH_3NH_3PbI_3$/PTB7-Th/MoO_3/Ag and ITO/sol-gel ZnO/PCBM/$CH_3NH_3PbI_3$/PTB7-Th/MoO_3/Ag. The current density-voltage (J-V) characteristics of the devices under AM 1.5 G irradiation with an irradiation intensity of 100 mW cm^{-2} and external quantum efficiency (EQE) spectra are shown in Figure 3a and b, respectively. The photovoltaic parameters of these devices are summarized in Table 1. As shown in Figure 3a, the device with a sol-gel ZnO film exhibited a PCE of 8.37% with a short-circuit current density (Jsc) of 14.31 mA cm^{-2}, an open circuit voltage (V_{oc}) of 0.86 V, and a fill factor (FF) of 68%. The performances are comparable to those of perovskite solar cells incorporating ZnO NPs which were synthesized by the previously reported method.[3](see supporting information Figure S8)

On the other hand, the perovskite solar cells containing sol gel ZnO/PCBM showed remarkably enhanced device performance compared with that of the ZnO devices, resulting in the best PCE of 11.04% with J_{sc} ~ 15.10 mA cm^{-2}, V_{oc} ~ 1.03 V, and FF ~ 71%. Notably, the V_{oc} and FF values were further enhanced relative to those of the of ZnO devices. As indicated by the electronic structure of the films (see Figure 2), the enhancement in the device performance can be attributed to the following factors: the larger energy-level offset between the quasi Fermi levels of the ECL and the HTL adjacent to the perovskite absorber and the more favorable energy-level alignment between the CBM of ZnO/PCBM and the perovskite absorber for efficient electron collection, resulting in a high FF. When considering the perovskite solar cells incorporating only PCBM on ITO substrate exhibited poor device performances (see supporting information Figure S9), the synergic effect of ZnO and PCBM is crucial for improving device performances.

Table 1. Photovoltaic parameters under AM 1.5G solar spectrum with a light intensity of 100 mW·cm^{-2}.

Cathode (mean ± s.d.)	V_{oc} (V)	J_{sc} (mA cm^{-2})	FF	PCE (%) (Best)	R_s (Ω·cm^2)[a]
ITO/ZnO	0.78 ± 0.05	14.54 ± 0.16	0.68 ± 0.01	7.65 ± 0.47 (8.37)	9.0 ± 0.87
ITO/ZnO/PCBM	1.02 ± 0.01	14.73 ± 0.23	0.73 ± 0.02	10.87 ± 0.13 (11.04)	7.4 ± 0.25

[a] The R_s of the perovskite solar cells were calculated using $(dJ/dV)^{-1}$ at $V = V_{oc}$.

To further investigate the role of interfacial modification in enhancing the performance of the fabricated devices, we measured the light-intensity dependence of V_{oc} for the perovskite solar cells with ZnO and ZnO/PCBM ECLs, which describes the order of recombination processes in solar devices (see supporting information Figure S10).[23, 24] Figure 4a shows a

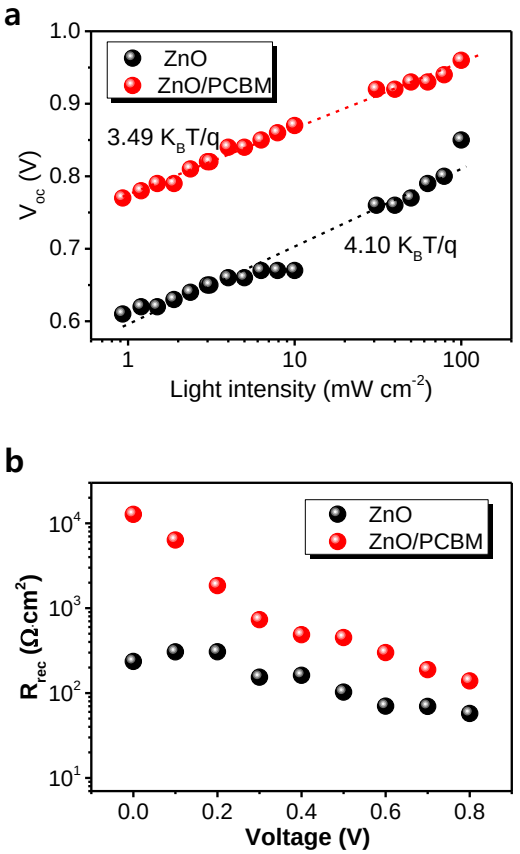

Figure 4. (a) Light-intensity dependence of the V_{oc} of the perovskite solar cells with ZnO and ZnO/PCBM. The lines represent the best fits to the data, for which the slope is indicated. (b) Recombination resistance at different applied biases extracted from IS characterization of the perovskite solar cells.

semi-logarithmic plot of V_{oc} as a function of light intensity for the devices and the slopes derived from the lines fitted linearly to the data. As shown in Figure 4a, the device with only ZnO shows a strong dependence of V_{oc} on the light intensity, with a slope of 4.10 k_BT/q, where k_B is Boltzmann's constant, q is the elementary charge, and T is temperature in Kelvin. However, when the ZnO is modified with PCBM, the device shows a lower slope of 3.49 k_BT/q, indicating reduced trap-assisted recombination in the devices.[17, 25] The slope of our perovskite solar cells is similar with previously reported values of $CH_3NH_3PbI_3$ perovskite devices but slightly higher than that of mixed halide ($CH_3NH_3PbI_{3-x}Cl_x$) perovskite solar cells.[26-28] We speculate that the differences can be related with perovskite composition, because the exciton diffusion length and charge dynamics were significantly affected by doping Cl ions into $CH_3NH_3PbI_3$ perovskite.[6, 29]

It is noted that the slopes of the $CH_3NH_3PbI_3$-based PHJ perovskite solar cells are relatively larger than those of polymer solar cells (PSCs) (~ k_BT/q) and solid-state, dye-sensitized solar cells (SDSSCs) (~ 1.7 k_BT/q); this finding suggests that the dominant charge recombination mechanism of the perovskite

solar cells at the open-circuit voltage is monomolecular recombination, which is distinguished from bimolecular recombination in PSCs and a combination of monomolecular and bimolecular recombination in SDSSCs at the open-circuit voltage.[30, 31]

Monomolecular recombination, also referred to as Shockley-Read-Hall (SRH) recombination, is a first-order recombination process in which electrons and holes recombine through trap sites in the bulk of an absorber or at interfaces in devices.[31, 32] By surface modification using the fullerene derivative, we expect that the trap sites in the ZnO film were significantly reduced, thereby enhancing the device performance. Although the trap-filling mechanism is not clearly understood at this moment, we speculate that there are some charge transfer reactions that occur from the PCBM to ZnO due to the difference in the WF or a chemical interaction that fills the trap sites in the ZnO.[18, 33] To further reveal the trap-filling mechanism is beyond the scope of this work, and study of the mechanism is underway in our laboratory.

The charge recombination processes were also investigated by extracting the recombination resistance (R_{rec}) from impedance spectroscopy (IS) measurements of the perovskite solar cells. Generally, the features observed in the low-frequency region in the IS spectra are closely related with charge recombination processes, and the R_{rec} is obtained by fitting the Nyquist plots in this region.[34, 35] Figure 4b shows the R_{rec} values of the perovskite solar cells with ZnO and ZnO/PCBM at different applied voltages under 1-sun illumination. As shown in Figure 4b, the device with ZnO/PCBM exhibited higher R_{rec} values (lower recombination rate) compared to those of the device containing only ZnO at low applied bias, indicating that surface charge recombination was significantly suppressed by the interfacial modification.[36] Interestingly, the interfacial modification of ZnO also decreased the extent of bulk charge recombination, which corresponds to the higher R_{rec} values obtained at high applied bias.[37] We speculate that the reduced bulk charge recombination is attributed to an increased built-in potential, due to the modified electronic structure of the ZnO/PCBM substrate, which facilitated more efficient sweeping of photo-generated charge carriers.[17] Therefore, based on the light-intensity dependence of Voc and the IS measurements, it is confirmed that the interfacial modification of the ZnO substrate with PCBM significantly reduced trap-assisted charge recombination at the interfaces as well as in the absorber of the devices, thereby enhancing the device performance.

To further optimize the perovskite solar cells, we incorporated 2,2′,7,7′-tetrakis(N,N- di-p-methoxyphenylamine)-9,9′-spirobifluorene (spiro-OMeTAD) as the HTL which is the most widely used organic transport layer in SDSSCs and perovskite solar cells due to its excellent optical transparency in the visible range.[38, 39] Figure 5 shows the current density-voltage (J-V) characteristics of the devices with a structure of

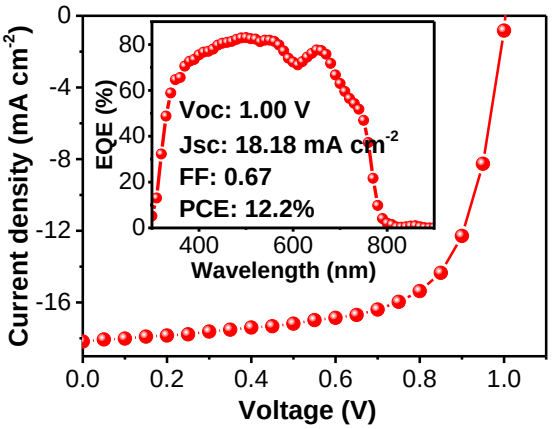

Figure 5. (a) Current density-voltage characteristics of the best planar-heterojunction perovskite solar cells with a structure of ITO/ZnO/PCBM/$CH_3NH_3PbI_3$/spiro-OMeTAD/MoO_x/Ag measured under AM 1.5G irradiation at 100 mW cm^{-2}. EQE spectrum of the device is shown in the inset.

ITO/ZnO/PCBM/$CH_3NH_3PbI_3$/sprio-OMeTAD/MoO_3/Ag, under AM 1.5 G irradiation with irradiation intensity of 100 mW cm^{-2} and the corresponding external quantum efficiency (EQE) spectrum (inset). As shown in Figure 5, the PHJ perovskite solar cell showed a very high PCE of 12.2% with a J^{sc} of 18.18 mA cm^{-2}, V_{oc} of 1.00 V, and FF of 67%. The outperforming efficiency of the spiro-OMeTAD device compared to the efficiency of the PTB7-Th device of PTB7-Th is attributed to the higher J_{sc}, which is mainly derived from efficient light harvesting with EQE values approaching 80% over the wavelength range of 400 ~ 650 nm, as shown in the inset of Figure 5. It is noteworthy that the results obtained for our optimized device are among the best reported for state-of-the-art low-temperature solution-processed photovoltaics.

Conclusions

In conclusion, we successfully demonstrated efficient PHJ perovskite solar cells with a high PCE of 12.2% by fine-tuning the interfacial properties of a sol-gel-processed ZnO ECL using PCBM as an organic surface modifier. By depositing PCBM onto the ZnO film, the V_{oc} values of the devices with ZnO/PCBM substrates increased to ~ 1.03 V compared to the Voc of ~ 0.83 V measured for devices with only ZnO due to the modified electronic structure of the ZnO layer, as evidenced by the results of photoelectron spectroscopy analysis. In addition, trap-assisted charge recombination at the interface of ZnO and in the bulk of the perovskite absorber was effectively suppressed by the interfacial modification, thereby improving the performance of the devices. These results highlight the importance of interfacial engineering as a new strategy for improving the PCEs of planar-structured perovskite solar cells. By further optimization and by pursuing a rational interfacial engineering design, we expect that greater performance enhancements can be achieved in the near future.

Acknowledgements

This work was supported by the Core Technology Development Program for Next-Generation Solar Cells of the Research Institute for Solar and Sustainable Energies (RISE) at GIST and the National Research Foundation (NRF) of Korea (NRF-2014R1A2A1A09006137). We also acknowledges the support provided by the National Research Foundation of Korea (NRF) grant funded by the Korea government (MSIP) (No. 2008-0062606, CELA-NCRC).

Notes and references

[a] Department of Nanobio Materials and Electronics, Gwangju Institute of Science and Technology, Gwangju 500-712, Republic of Korea.

[b] School of Materials Science and Engineering, Gwangju Institute of Science and Technology, Gwangju 500-712, Republic of Korea.

[c] Heeger Center for Advanced Materials & Research Institute for Solar and Sustainable Energies, Gwangju Institute of Science and Technology, Gwangju 500-712, Republic of Korea.

† Footnotes should appear here. These might include comments relevant to but not central to the matter under discussion, limited experimental and spectral data, and crystallographic data.

Electronic Supplementary Information (ESI) available: [details of any supplementary information available should be included here]. See DOI: 10.1039/c000000x/

1. M. Liu, M. B. Johnston and H. J. Snaith, *Nature*, 2013, **501**, 395-398.
2. J. Burschka, N. Pellet, S.-J. Moon, R. Humphry-Baker, P. Gao, M. K. Nazeeruddin and M. Gratzel, *Nature*, 2013, **499**, 316-319.
3. D. Liu and T. L. Kelly, *Nat. Photon.*, 2014, **8**, 133-138.
4. P.-W. Liang, C.-Y. Liao, C.-C. Chueh, F. Zuo, S. T. Williams, X.-K. Xin, J. Lin and A. K. Y. Jen, *Adv. Mater.*, 2014, n/a-n/a.
5. G. Xing, N. Mathews, S. Sun, S. S. Lim, Y. M. Lam, M. Grätzel, S. Mhaisalkar and T. C. Sum, *Science*, 2013, **342**, 344-347.
6. S. D. Stranks, G. E. Eperon, G. Grancini, C. Menelaou, M. J. P. Alcocer, T. Leijtens, L. M. Herz, A. Petrozza and H. J. Snaith, *Science*, 2013, **342**, 341-344.
7. J. H. Noh, S. H. Im, J. H. Heo, T. N. Mandal and S. I. Seok, *Nano Lett.*, 2013, **13**, 1764-1769.
8. Q. Chen, H. Zhou, Z. Hong, S. Luo, H.-S. Duan, H.-H. Wang, Y. Liu, G. Li and Y. Yang, *J. Am. Chem. Soc.*, 2013, **136**, 622-625.
9. G. E. Eperon, V. M. Burlakov, P. Docampo, A. Goriely and H. J. Snaith, *Adv. Funct. Mater.*, 2014, **24**, 151-157.
10. J. T.-W. Wang, J. M. Ball, E. M. Barea, A. Abate, J. A. Alexander-Webber, J. Huang, M. Saliba, I. Mora-Sero, J. Bisquert, H. J. Snaith and R. J. Nicholas, *Nano Lett.*, 2013, **14**, 724-730.
11. K. Wojciechowski, M. Saliba, T. Leijtens, A. Abate and H. J. Snaith, *Energy & Environmental Science*, 2014, **7**, 1142-1147.
12. J. M. Ball, M. M. Lee, A. Hey and H. J. Snaith, *Energy & Environmental Science*, 2013, **6**, 1739-1743.
13. W. J. E. Beek, M. M. Wienk, M. Kemerink, X. Yang and R. A. J. Janssen, *The Journal of Physical Chemistry B*, 2005, **109**, 9505-9516.
14. Z. E. Allouni, M. R. Cimpan, P. J. Høl, T. Skodvin and N. R. Gjerdet, *Colloids and Surfaces B: Biointerfaces*, 2009, **68**, 83-87.
15. M. R. Arefi and S. Rezaei-Zarchi, *International Journal of Molecular Sciences*, 2012, **13**, 4340-4350.
16. Y. Sun, J. H. Seo, C. J. Takacs, J. Seifter and A. J. Heeger, *Adv. Mater.*, 2011, **23**, 1679-1683.
17. A. K. K. Kyaw, D. H. Wang, V. Gupta, J. Zhang, S. Chand, G. C. Bazan and A. J. Heeger, *Adv. Mater.*, 2013, **25**, 2397-2402.
18. S.-H. Liao, H.-J. Jhuo, Y.-S. Cheng and S.-A. Chen, *Adv. Mater.*, 2013, **25**, 4766-4771.
19. M. C. Gwinner, R. D. Pietro, Y. Vaynzof, K. J. Greenberg, P. K. H. Ho, R. H. Friend and H. Sirringhaus, *Adv. Funct. Mater.*, 2011, **21**, 1432-1441.
20. M. Kröger, S. Hamwi, J. Meyer, T. Riedl, W. Kowalsky and A. Kahn, *Appl. Phys. Lett.*, 2009, **95**, 123301-1-3.
21. M. M. Lee, J. Teuscher, T. Miyasaka, T. N. Murakami and H. J. Snaith, *Science*, 2012, **338**, 643-647.
22. S. Ryu, J. H. Noh, N. J. Jeon, Y. C. Kim, W. S. Yang, J. W. Seo and S. I. Seok, *Energy & Environmental Science*, 2014.
23. L. J. A. Koster, V. D. Mihailetchi, R. Ramaker and P. W. M. Blom, *Appl. Phys. Lett.*, 2005, **86**, -.
24. M. Lenes, S. W. Shelton, A. B. Sieval, D. F. Kronholm, J. C. Hummelen and P. W. M. Blom, *Adv. Funct. Mater.*, 2009, **19**, 3002-3007.
25. S. R. Cowan, W. L. Leong, N. Banerji, G. Dennler and A. J. Heeger, *Adv. Funct. Mater.*, 2011, **21**, 3083-3092.
26. D. Bi, S.-J. Moon, L. Haggman, G. Boschloo, L. Yang, E. M. J. Johansson, M. K. Nazeeruddin, M. Gratzel and A. Hagfeldt, *RSC Advances*, 2013, **3**, 18762-18766.
27. D. Bi, G. Boschloo, S. Schwarzmuller, L. Yang, E. M. J. Johansson and A. Hagfeldt, *Nanoscale*, 2013, **5**, 11686-11691.
28. J. You, Z. Hong, Y. Yang, Q. Chen, M. Cai, T.-B. Song, C.-C. Chen, S. Lu, Y. Liu and H. Zhou, *ACS Nano*, 2014, **8**, 1674-1680.
29. N. J. Jeon, J. H. Noh, Y. C. Kim, W. S. Yang, S. Ryu and S. I. Seok, *Nat. Mater.*, 2014, **advance online publication**.
30. H. J. Snaith, L. Schmidt-Mende, M. Grätzel and M. Chiesa, *Phys. Rev. B*, 2006, **74**, 045306.
31. S. R. Cowan, A. Roy and A. J. Heeger, *Phys. Rev. B*, 2010, **82**, 245207.
32. D. Credgington, F. C. Jamieson, B. Walker, T.-Q. Nguyen and J. R. Durrant, *Adv. Mater.*, 2012, **24**, 2135-2141.
33. H. Ma, H.-L. Yip, F. Huang and A. K. Y. Jen, *Adv. Funct. Mater.*, 2010, **20**, 1371-1388.
34. V. Gonzalez-Pedro, E. J. Juarez-Perez, W.-S. Arsyad, E. M. Barea, F. Fabregat-Santiago, I. Mora-Sero and J. Bisquert, *Nano Lett.*, 2014, **14**, 888-893.
35. A. Dualeh, T. Moehl, N. Tétreault, J. Teuscher, P. Gao, M. K. Nazeeruddin and M. Grätzel, *ACS Nano*, 2013, **8**, 362-373.
36. E. J. Juarez-Perez, M. Wuβler, F. Fabregat-Santiago, K. Lakus-Wollny, E. Mankel, T. Mayer, W. Jaegermann and I. Mora-Sero, *The Journal of Physical Chemistry Letters*, 2014, **5**, 680-685.
37. B. Suarez, V. Gonzalez-Pedro, T. S. Ripolles, R. S. Sanchez, L. Otero and I. Mora-Sero, *The Journal of Physical Chemistry Letters*, 2014, **5**, 1628-1635.
38. J. H. Noh, N. J. Jeon, Y. C. Choi, M. K. Nazeeruddin, M. Gratzel and S. I. Seok, *Journal of Materials Chemistry A*, 2013, **1**, 11842-11847.
39. D. Bi, L. Yang, G. Boschloo, A. Hagfeldt and E. M. J. Johansson, *The Journal of Physical Chemistry Letters*, 2013, **4**, 1532-1536.

Graphics for Contents

Efficient Planar-Heterojunction Perovskite Solar Cells Achieved via Interfacial Modification of Sol-gel ZnO Electron Collection Layer

Junghwan Kim,[a] Geunjin Kim,[b] Tae Kyun Kim,[c] Sooncheol Kwon,[a] Hyungcheol Back,[b] Jinho Lee,[a] Seoung Ho Lee,[c] Hongkyu Kang[b] and Kwanghee Lee*[a,b,c]

The importance of interfacial engineering as a new strategy for improving the power conversion efficiencies (PCEs) of planar-heterojunction (PHJ) perovskite solar cells is highlighted by incorporating sol-gel ZnO modified with PCBM.